JOURNAL OF PETROLOGY | VOLUME 43 | NUMBER 6 | PAGES 943–962 | 2002

Petrogenesis of the Anorthosite Dyke Swarm of Tromsø, North Norway: Experimental Evidence for Hydrous Anatexis of an Alkaline Mafic Complex

RUNE S. SELBEKK* AND KJELL P. SKJERLIE

DEPARTMENT OF GEOLOGY, UNIVERSITY OF TROMSØ, DRAMSVEIEN 201, N-9037 TROMSØ, NORWAY

RECEIVED APRIL 27, 2001; REVISED TYPESCRIPT ACCEPTED DECEMBER 5, 2001

The 456 ± 4 Ma Skattøra migmatite complex in the north Norwegian Caledonides consists of migmatitic nepheline-normative metagabbros and amphibolites that are net-veined by numerous nepheline-normative anorthositic and leucodioritic dykes. Plagioclase ($An_{20–50}$) is the dominant mineral (85–100%) in the dykes and the leucosome, but amphibole is generally present in amounts up to 15%. The following observations strongly suggest formation of the anorthositic magma by anatexis of the surrounding gabbro in the presence of an H_2O-bearing fluid phase: (1) the migmatites have plagioclase-rich (anorthositic) leucosomes and amphibole-rich restites; (2) crystallization of amphibole in the anorthositic and leucodioritic dykes suggests high H_2O activity; (3) the presence of coarse-grained to pegmatitic dykes and miarolitic cavities indicates a fluid-rich magma; (4) hydration zones that surround many anorthosite dykes suggest that the magma probably expelled H_2O-rich fluids during crystallization. Water-saturated melting experiments at 0·5–1·5 GPa and temperatures from 800 to 1000°C have been performed on a nepheline-normative gabbro to test the proposed petrogenesis of the Skattøra anorthosites. The glasses produced close to the solidus are tonalitic in composition, but they become richer in plagioclase at higher temperatures. At and below 1·0 GPa, the residues are composed of amphibole. Experiments above 1·0 GPa produced residual garnet and/or zoisite in addition to amphibole, suggesting that the anorthositic dykes in the Skattøra migmatite complex formed below 1·25 GPa. The experiments show that the high Na_2O content of the anorthosite dykes can only be produced if Na is added to the charges. The glass that best fits the composition of the Skattøra dykes was produced at 1·0 GPa and 900°C with 2 wt % Na(OH) added.

KEY WORDS: *anorthosite; dyke swarm; anatexis; experimental petrology*

INTRODUCTION

At present, anorthosites can be classified into at least five separate types: Archaean megacrystic (e.g. Ashwal, 1993); Proterozoic massif-type (e.g. Simmons & Hanson, 1978; Taylor *et al.*, 1984; Emslie, 1985; Duchesne *et al.*, 1999; Longhi *et al.*, 1999); layered mafic intrusions; oceanic (e.g. Ashwal, 1993); hydrous anorthosites (Selbekk *et al.*, 2000). The first four types of anorthosite are thought to have formed by crystallization of residual melts formed by fractional crystallization from dry melts, because of their anhydrous mafic mineralogy, whereas the hydrous anorthosites are believed to form by anatexis of plagioclase-rich rocks in the presence of an H_2O-rich fluid phase (Oliver, 1977; Fershtater *et al.*, 1998; Selbekk *et al.*, 2000).

Oliver (1977) suggested that some anorthositic pegmatites and veins in New Zealand formed by anatexis of feldspathic hornblende granulites in the presence of an H_2O-bearing fluid phase. Fershtater *et al.* (1998) described hornblende-bearing anorthositic dykes from the Ural platinum-bearing belt, and suggested that these anorthosites are generated by anatexis in the presence of an H_2O-rich fluid phase. These anorthosites are quartz free and indicate unusual anatectic conditions, as melts produced under normal conditions of anatexis should be granitic in composition. Selbekk *et al.* (2000) suggested that the nepheline-normative anorthosite dyke swarm in the Skattøra migmatite complex (SMC) in the Caledonides of northern Norway (Fig. 1) formed by anatexis of nepheline-normative gabbros in the presence of an

*Corresponding author. E-mail: runes@ibg.uit.no

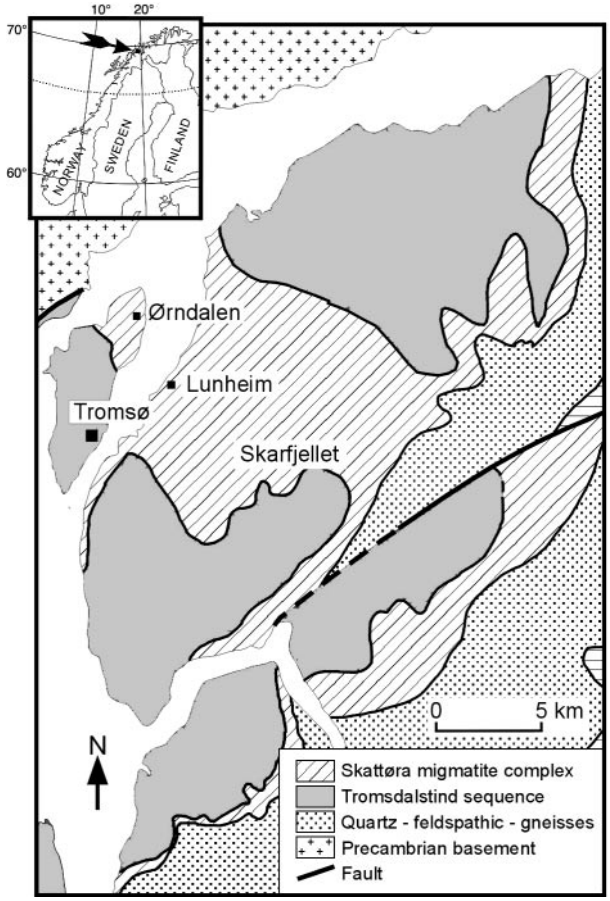

Fig. 1. Geological map of the Tromsø area, simplified from Krogh *et al.* (1990) and Zwaan *et al.* (1998), showing the Skattøra migmatite complex.

H_2O-bearing fluid phase. This conclusion was supported by field relations, geochemistry and preliminary high-pressure experiments. They also suggested that these anorthosites should be called 'hydrous anorthosites', as they contain hydrous mafic phases and clearly have an origin different from most other anorthosites (Selbekk *et al.*, 2000).

Anorthosite dykes have rarely been described (Kolderup, 1933; Wiebe, 1979; Jafri & Saxena, 1981; Leelanandam & Reddy, 1990; Fershtater *et al.*, 1998; Selbekk *et al.*, 2000), and to our knowledge the SMC is the only anorthositic dyke complex known. The main purpose of this paper is to present the results of H_2O-saturated melting experiments on a nepheline-normative gabbro. These experiments have been performed to test the hypothesis that the SMC anorthosites formed by partial melting of alkaline gabbro in the presence of a hydrous fluid phase.

REGIONAL GEOLOGICAL SETTING

The Troms segment of the Scandinavian Caledonides is characterized by a series of flat-lying nappes and nappe complexes that were emplaced from WNW (Binns, 1978; Andresen *et al.*, 1985). Of the various nappe complexes, the most important for the present problem are the Lyngen, Nakkedal and Tromsø Nappes (Zwaan *et al.*, 1998). The Lyngen Nappe is dominated by the 469 $\pm$ 5 Ma Lyngen magmatic complex, which is suggested to represent the fore-arc part of an island-arc system (Furnes & Pedersen, 1995; Oliver & Krogh, 1995; Selbekk *et al.* 1998), unconformably overlain by the Balsfjord group with late Ordovician to Silurian fossils (Bjørlykke & Olaussen, 1981).

The Nakkedal Nappe is positioned above the Lyngen Nappe and consists of metasedimentary rocks, predominantly quartzo-feldspathic gneisses, and the SMC. The contact between the quartzo-feldspathic gneisses and the SMC is gradational, and is cross-cut by numerous leucodioritic to anorthositic dykes (Fig. 2) (Landmark, 1951, 1973). An anorthosite dyke and a leucosome in the SMC have been dated by the U/Pb method on titanite to 456 $\pm$ 4 Ma (Selbekk *et al.*, 2000). The age of the protolith to the anorthosites in the SMC is unknown.

The boundary between the SMC and the overlying high-pressure rocks of the Tromsø Nappe is tectonic, often strongly mylonitized, and none of the anorthositic dykes are seen to cut the contact or the rocks of the Tromsø Nappe (Andresen *et al.*, 1985; Krogh *et al.*, 1990). The Tromsø nappe consists of partly retrograded eclogites intimately associated with pelitic to semipelitic schists, marbles, calc-silicate rocks, metabasites, ultramafites and gneisses (Krogh *et al.*, 1990). Some of the eclogites also show migmatite with tonalitic leucosomes and melanosomes with garnet and amphiboles. These migmatites have been dated by U/Pb method on titanite to 458 Ma (K. P. Skjerlie, personal communication, 2001).

GENERAL GEOLOGY OF THE SKATTØRA MIGMATITE COMPLEX

The SMC (Fig. 1) is composed mainly of migmatitic mafic rocks with anorthositic to leucodioritic leucosomes and mesosomes of amphibolite. It locally contains lenses of migmatized metagabbro, serpentinite and metasediments (Selbekk *et al.*, 2000).

The migmatites vary from metatexites to diatexites, according to the terminology of Mehnert (1968) and Ashworth (1985) (Fig. 2). Low-melt areas contain small foliation-parallel leucosomes, but irregular patches of leucosome also occur. The leucosomes and melanosomes often form concordant bands, and the boundary between them varies from sharp and parallel to more

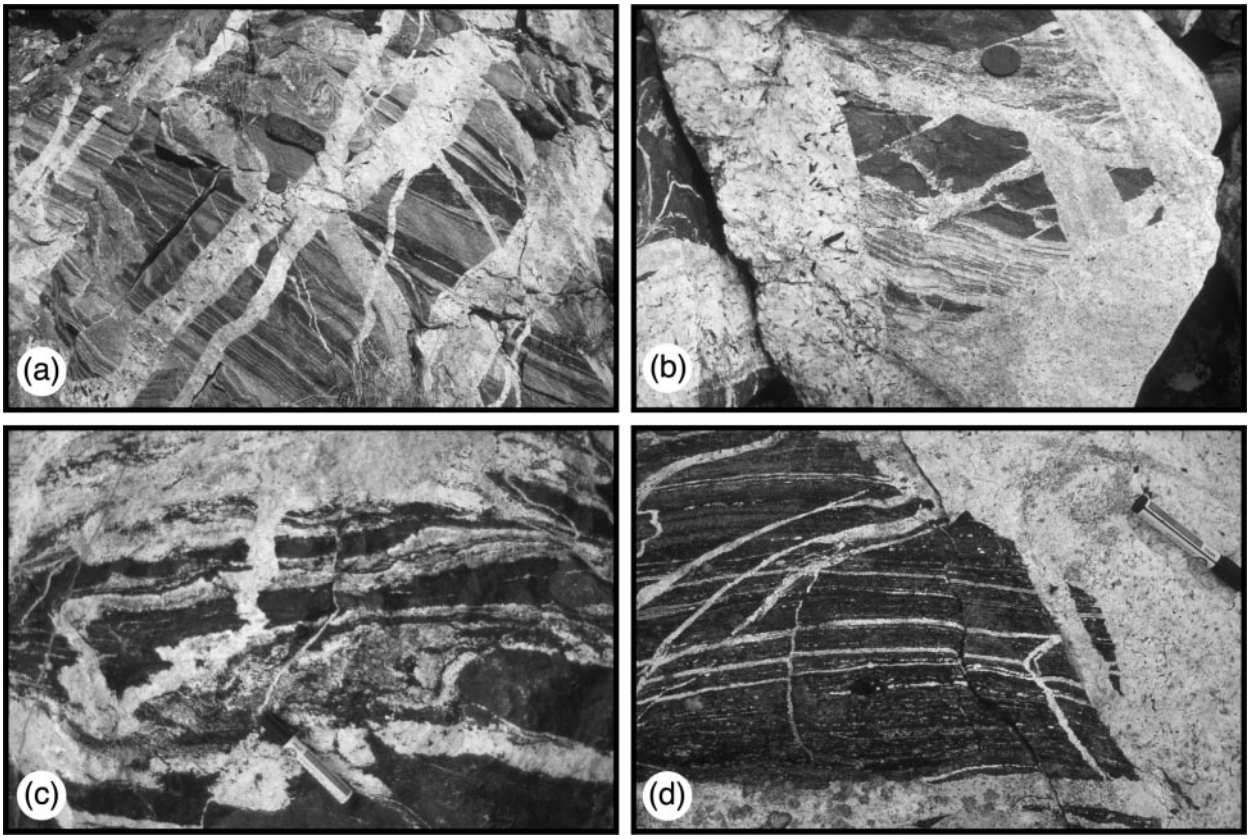

Fig. 2. (a) Anorthositic dykes cross-cutting the SMC at Ørndalen. Lens cap 6 cm. (b) Anorthositic dykes cross-cutting a migmatite zone at Lunheim. Same scale as for (a). (c) Metatexitic to diatexitic migmatite with disrupted restite–amphibole layers. From the quarry at Lunheim. Pencil is 13 cm long. (d) Amphibolitic restite, showing melt draining out of the migmatite. From the quarry at Lunheim. Same scale as for (c).

irregular and diffuse. High-melt areas form stromatic to schlieric migmatites. In some areas the melt fraction was so high that the migmatite layering was disrupted. The migmatites exhibit drain-out structures, where melts migrated first along grain boundaries into hairline cracks that are connected to large dykes, and the migmatite complex thus has the appearance of a dyke-root system.

Characteristic of the SMC is net-veining by numerous anorthosite dykes (Fig. 2); the proportion of dykes ranges up to 90%, with an average of ~50%. Dyke thicknesses vary from a few centimetres to several metres. In general, the dykes cross-cut the foliation, but they can also be concordant with the foliation. In places dykes form an anastomosing network, but larger dykes are usually straight. In most cases the dykes have sharp and rather planar contacts with the country rocks, but dykes with more diffuse and irregular borders also occur. Thicker dykes usually dip steeply and cut the foliation. Work in progress suggests that the orientation of the dykes is compatible with intrusion in a coaxial stress field.

PETROGRAPHY

The dykes have a modal composition of 85–100% plagioclase ($An_{20–50}$) and 0–15% irregularly distributed amphibole (pargasite to ferropargasite). The dykes vary from fine grained to pegmatitic with plagioclase and amphibole crystals up to 10 and 15 cm in length, respectively. Plagioclase crystals are generally unzoned and crystals from a single dyke have relatively uniform compositions. The plagioclase crystals are subhedral, and large crystals have fluid inclusions.

Along the margins, amphibole crystals are commonly orientated roughly perpendicular to the dyke walls. In the central parts of dykes, the amphibole crystals are frequently randomly orientated. Some dykes have amphibole crystals only along the margins and no amphibole in the centre. Other dykes have a more uniform distribution of amphibole. Some dykes contain amphibole crystals orientated in repeated bands perpendicular to the wall; other coarse-grained anorthosites show epitaxial growth of plagioclase and amphibole.

Accessory minerals in the dykes are apatite, muscovite, biotite, iron oxides or sulphides, titanite and epidote or

clinozoisite. Quartz has not been observed. Miarolitic cavities with crystals of plagioclase, amphibole, calcite, prehnite and zeolite minerals (e.g. stilbite, heulandite) are common.

Lenses of metagabbro consist of 0–65% plagioclase ($An_{72–90}$) and 35–100% amphibole, and are usually medium grained to pegmatitic. The plagioclase is generally saussuritized. The metagabbro shows an inequigranular texture, without any preferred crystal orientation, but locally modal layering occurs. Accessory minerals are Fe–Ti oxides, sulphides and titanite.

The amphibolites consist of 70–100% amphibole, 0–30% plagioclase, and 0–5% Fe–Ti oxide. They are usually medium to coarse grained and show nematoblastic textures. The amphibole grains are subhedral to anhedral. Most amphibolites are interpreted to represent restites, but a few that are parallel to dyke margins are probably hydration zones caused by dewatering of the anorthositic melt during crystallization.

EVIDENCE FOR ANATEXIS IN THE PRESENCE OF AN H_2O-BEARING FLUID

The following observations strongly suggest formation of the dyke magma by anatexis of the surrounding gabbro in the presence of an H_2O-bearing fluid phase: (1) the migmatites have plagioclase-rich (anorthositic) leucosomes and amphibole-rich restites; experimental studies have shown that H_2O-rich anatexis of metabasalt stabilizes amphibole and destabilizes plagioclase (e.g. Yoder & Tilley, 1962; Beard & Lofgren, 1991; Patiño Douce & Harris, 1998); (2) crystallization of amphibole in the anorthositic and leucodioritic dykes suggests high H_2O activity (De Waard, 1969); (3) the presence of coarse-grained to pegmatitic dykes and miarolitic cavities indicates a fluid-rich magma; (4) hydration zones that surround many anorthosite dykes suggest that the magma probably expelled H_2O-rich fluids during crystallization; (5) fluid inclusions in plagioclase in the dykes consist of three phases, liquid, vapour and an isotropic colorless solid phase, probably halite. The average geochemical composition of 17 anorthositic dykes is presented in Table 1.

Table 1: Average chemical composition of anorthositic dykes in the Skattøra migmatite complex

	Average* anorthosite	Minimum value	Maximum value
SiO_2	58·21	53·91	61·39
TiO_2	0·25	0·07	0·65
Al_2O_3	23·02	21·66	24·47
FeO^t	1·85	0·56	3·96
MnO	0·03	0·01	0·05
MgO	0·75	0·23	1·52
CaO	6·38	4·60	8·82
Na_2O	7·69	6·02	9·03
K_2O	0·21	0·16	0·33
P_2O_5	0·08	0·02	0·28
LOI	0·41		
Total	98·89		
Sr	1352	1085	1483
Y	4	—	10
Zr	89	—	347
Ba	109	80	141
Fe/(Fe + Mg)	0·71	0·63	0·78

*Average composition of 17 anorthosites and leucodiorites from the Skattøra migmatite complex.
—, not determined; FeO^t, total iron as FeO; LOI, loss on ignition.

PREVIOUS EXPERIMENTAL STUDIES ON PLAGIOCLASE MELTING

Yoder & Tilley (1962) studied crystallization sequences in various basalt liquids under conditions of $P_{H_2O} = P_{total}$ up to 1·0 GPa. They observed that plagioclase was the last phase to crystallize, implying that the first liquid formed during melting should be plagioclase rich. Fram & Longhi (1992) suggested that plagioclase–melt partitioning is a strong function of pressure. The presence of an H_2O-bearing fluid phase is known to lower the solidus temperature of rocks (e.g. Johannes, 1978; Johannes & Holz, 1996). Dry melting of plagioclase occurs between 1100°C and 1500°C depending on the plagioclase composition (Johannes, 1978; Hall, 1987). However, in the presence of an H_2O-bearing fluid phase, the melting temperature is lowered to ~750–1200°C at 0·5 GPa (Johannes, 1978). Plagioclase–melt equilibria are strongly dependent on both the temperature and the H_2O content of the melt (Housh & Luhr, 1991). Melts in equilibrium with plagioclase, particularly high-An feldspars, will be relatively enriched in plagioclase components at high H_2O contents (Conrad *et al.*, 1988). As shown by earlier workers, the presence of a fluid phase with high H_2O activity stabilizes hydrous mafic phases such as amphibole and micas and destabilizes plagioclase and quartz during partial melting (e.g. Yoder & Tilley, 1962; Beard & Lofgren, 1989, 1990; Patiño Douce & Harris, 1998).

CHARACTERIZATION OF THE STARTING MATERIAL

Water-saturated experiments were performed on a nepheline-normative (Ne = 2·8) metagabbro (109SD) from the Rognsund Intrusion (Robins, 1982) within the Seiland Igneous Province of north Norway, kindly provided by Professor B. Robins. The reason for using the Rognsund gabbro instead of a sample from the SMC is that the lenses of SMC metagabbro are all severely recrystallized, and may have modified compositions compared with the original starting material. Most of them have probably been melted. The hypothesis we want to test is that the anorthosite dykes formed by H_2O-fluxed melting of silica-undersaturated gabbro, and thus we chose a convenient nepheline-normative gabbro.

The bulk chemical composition and mineral chemistry of the selected starting material are presented in Table 2. The modal composition of the sample is 57% pargasitic amphibole, 41% plagioclase (An_{70-84}), and 2% ilmenite and apatite. The chemical composition of the starting material BR 109SD is compared with the average chemical composition of the five least altered metagabbros in the Skattøra migmatite complex in Table 3.

Cs(OH) (1 wt %) was added to the starting material to enhance the contrast between the melt and the plagioclase crystals because they are otherwise similar in appearance in back-scattered electron images. During the experiments, Cs was enriched in the glass as expected, but no Cs(OH) entered the plagioclase and no Cs-rich phases formed. Newly grown amphibole contains a maximum of 0·5 wt % Cs.

In one of the run series, 2 wt % Na(OH) was added to the starting material to study how sodium affects the melt composition and residue. These experiments were performed because the H_2O-saturated experiments did not reproduce the Na_2O content of the SMC anorthosite dykes. In nature, a saline fluid phase, for example, subducted seawater, may have been involved in the melting event (e.g. Selbekk *et al.*, 2002). Na(OH) was chosen as the source of Na instead of NaCl to avoid crystallization of scapolite.

Water-saturated experiments with 10% albite (AL-1) added were performed to test whether the Na_2O content of the anorthositic dykes could be reproduced by increasing the Ab/An ratio of the starting material.

Table 2: Characterization of starting material BR 109SD

	Bulk rock* 109SD	Plagioclase†	Amphibole	Ilmenite
SiO_2	46·20	50·86	41·26	
TiO_2	2·05		2·47	49·44
Al_2O_3	20·40	31·35	12·99	
FeO^t	10·80		16·02	49·32
MnO	0·15		0·30	0·94
MgO	4·50		9·87	0·45
CaO	12·10	14·78	11·76	
Na_2O	3·02	3·50	2·38	
K_2O	0·33	0·07	0·87	
P_2O_5	0·06			
Total	99·61	100·56	97·92	100·15
CIPW norm				
Or	2·0			
Ab	20·4			
An	41·1			
Ne	2·8			
Di	15·3			
Ol	11·2			
Mt	1·9			
Il	3·9			
Ap	0·1			

*Values from Robins (1982).
†An content in the starting material based on the average of eight microprobe analyses is An_{70}.

EXPERIMENTAL AND ANALYTICAL PROCEDURES

Gold capsules were filled with sample ground to <10 μm, mixed with 1% Cs(OH), and 5–10% H_2O. The capsules were carefully inspected and weighed before and after welding, and after the run. Piercing of the capsule after the run resulted in outpouring of water, confirming water saturation during the run. The experiments were performed in NaCl–MgO–cell assemblies in a 0·5 inch, end-loaded piston-cylinder apparatus at the Department of Geology, University of Tromsø.

The capsules were enclosed in NaCl that acted as the pressure-transmitting medium in NaCl–MgO–graphite cells. The oil pressure in the hydraulic rams was measured by electronic pressure transducers and monitored by Maywood Instruments D3000-FPT digital controllers. The measured oil pressure was converted to sample pressure by the ratio of ram to piston areas and is assumed to be accurate to within 50 MPa.

Run times for the experiments ranged from 31 to 77 h (Table 4). Temperature was controlled to within ±5°C with a Eurotherm 808 regulator attached to a type C ($W_{74}Rh_{26}/W_{95}Rh_5$) thermocouple.

The f_{O_2} acting on the sample during an experiment influences the stability of Fe-bearing phases. Our samples

Table 3: Chemical composition of the starting material BR 109SD compared with average chemical composition of five metagabbros in the Skattøra migmatite complex

	Bulk rock* 109SD	Average metagabbro	Minimum value	Maximum value
SiO_2	46·20	47·64	45·45	49·17
TiO_2	2·05	1·37	0·29	2·15
Al_2O_3	20·40	18·65	16·46	21·03
FeO^t	10·80	10·13	5·01	13·45
MnO	0·15	0·14	0·10	0·17
MgO	4·50	5·74	3·91	8·99
CaO	12·10	10·31	7·38	13·56
Na_2O	3·02	4·03	2·61	4·98
K_2O	0·33	0·56	0·28	0·93
P_2O_5	0·06	0·10	0·02	0·31
Total	99·61	98·67		
CIPW norm				
Or	2·0	3·3		
Ab	20·4	24·0		
An	41·1	31·2		
Ne	2·8	5·5		
Di	15·3	15·9		
Ol	11·2	13·4		
Mt	1·9	1·8		
Il	3·9	2·6		
Ap	0·1	0·2		

*Values from Robins (1982).

contain amphibole, zoisite and garnet, and the stability of these phases will change as a function of f_{O_2}. We did not buffer our experiments by the use of the solid buffer two-capsule technique. However, in piston-cylinder experiments, it has repeatedly been shown that the f_{O_2} acting on the sample will be largely determined by the cell assembly because it is very much larger than the sample. Unfortunately, the phase assemblages produced in our experiments do not permit calculation of the f_{O_2}. On the basis of previous results, we assume that f_{O_2} is close to that generated by the quartz–fayalite–magnetite (QFM) solid buffer (Patiño Douce & Beard, 1995, 1996).

Analytical procedures and mode determination

Successful runs were polished for scanning electron microscope (University of Tromsø) and electron microprobe studies. Glass and mineral analyses were performed on a CAMECA CAMEBAX electron microprobe at the Geologisk Museum, University of Oslo. Natural and synthetic standards were used for calibration. Operating conditions were 10 nA and 15 kV. Glass and all phases except for zoisite were analysed with a rastered beam of size 5 μm × 5 μm to minimize sodium loss. Zoisite was analysed with a focused beam (1 μm) because of small grain size. Na and K were counted first, and Na was counted for 10 s. All other elements were counted for 20 s.

Na loss during microprobe analysis is particularly problematical in H_2O-rich granitic glasses (Patiño Douce & Harris, 1998). To determine the Na loss from our glasses we made H_2O-saturated glasses at 1·0 GPa from the international albite-rich standards JF-1 and AL-1. We then compared the microprobe analyses of the glasses with the recommended values of Govindaraju (1984, 1989). We found that elements other than sodium deviate by <0·5 wt %, except for SiO_2, which deviated by <1 wt %, from the recommended values. The Na losses in the glasses were 50–70%. We have therefore assumed 50% Na loss from the experimental glasses, which is similar to Na losses reported from other H_2O-rich experiments (e.g. Patiño Douce & Harris, 1998).

Phase abundances in the experimental run products were calculated by a combination of mass balance and partial estimates of modal abundances obtained from back-scattered electron images. It was not possible to calculate or otherwise obtain realistic modal values for the experiments at 900 and 950°C at 1·25 GPa, as a result of considerable melt segregation in the capsule. Calculated modes for the experiments and modal variations with temperature and pressure are given in Fig. 3.

APPROACH TO EQUILIBRIUM

Johannes (1978) concluded that it is not possible to reach equilibrium in the An–Ab–H_2O system in experiments performed around and below 800°C at 0·5 GPa because of low reaction rates. At 1000°C and 0·5 GPa equilibrium is reached within 1 h (Johannes, 1978). These results indicate that some of our low-temperature experiments may not have reached equilibrium. However, the neoformed phases in the experiments are generally homogeneous, both within single crystals and between crystals, suggesting that they have approached equilibrium. Disequilibrium features in the experiments are shown by garnets that show small variation in composition from core to margin. Garnets in the experiments are usually much larger than the other crystals, and the presence of inclusions of amphibole crystals in the garnet suggests that the garnet probably grew rapidly (Fig. 4). Euhedral

Table 4: Phase assemblages and experimental run conditions

T (°C)	*P* (GPa)	Duration (h)	Phase assemblage					
950	0·5	68	Prg	Pl	Ttn	Ilm	Gl	
850	0·7	67	Prg	Pl	Gl			
900	0·7	71	Prg	Pl	Ttn	Ilm	Gl	
950	0·7	78	Prg	Pl	Ttn	Ilm	Gl	
1000	0·7	48	Prg	Pl	Ilm	Gl		
850	1·0	72	Prg	Pl	Ttn	Gl		
900	1·0	71	Prg	Pl	Gl			
950	1·0	72	Prg	Pl	Ttn	Ilm	Cpx	Gl
975	1·0	70	Prg	Pl	Ttn	Ilm	Cpx	Gl
800	1·25	69	Prg	Pl	Zo	ilm	Gl	
825	1·25	73	Prg	Pl	Zo	Ilm	Gl	
850	1·25	72	Prg	Pl	Ttn	Ilm	Gl	
900	1·25	71	Prg	Pl	Grt	Ttn	Ilm	Gl
950	1·25	53	Prg	Pl	Grt	Ttn	Ilm	Gl
800	1·5	67	Prg	Zo	Grt	Ttn	Ilm	Gl
850	1·5	51	Prg	Zo	Grt	Ttn	Ilm	Gl
900	1·5	31	Prg	Zo	Grt	Ttn	Ilm	Gl
950	1·5	78	Prg	Zo	Grt	Ilm	Gl	
2% Na(OH)								
900	0·7	72	Prg	Pl	Ttn	Ilm	Gl	
850	1·0	73	Prg	Pl	Ttn	Ilm	Gl	
900	1·0	69	Prg	Pl	Ttn	Ilm	Gl	
950	1·0	73	Prg	Pl	Ttn	Ilm	Gl	
900	1·25	53	Prg	Pl	Zo	Ttn	Ilm	Gl
10% AL-1								
850	0·75	32	Prg	Ttn	Ilm	Gl		
900	0·75	80	Prg	Ttn	Ilm	Gl		
850	1·0	32	Prg	Ttn	Ilm	Gl		
900	1·0	72	Prg	Ttn	Ilm	Gl		

Prg, pargasite; Pl, plagioclase; Ttn, titanite; Ilm, ilmenite; Grt, garnet; Cpx, clinopyroxene; Zo, zoisite; Gl, glass (Kretz, 1983). Plagioclase and ilmenite are residual phases in all the experiments. Pargasite occurs both as residual and as a neoformed phase. The other minerals are all neoformed.

zoisite is always in contact with glass pools of homogeneous composition, suggesting that the zoisite was in equilibrium with the melt. The glasses show systematic compositional variations with pressure and temperature (Fig. 5), and are homogeneous throughout the experimental charges, even in near-solidus experiments with low melt fractions. Thus, despite the presence of some disequilibrium features, we conclude that the neoformed phases represent near-equilibrium assemblages.

EXPERIMENTAL RESULTS

Experimental conditions and phase assemblages in the experiments are listed in Table 4, and shown together with the approximate locations of the solidus and other phase boundaries in Fig. 6. The solidus is located on the basis of the presence or absence of glass in the experiments, but it is possible that minor amounts of glass were not detected in some experiments. Vesicles are filled with euhedral crystals close to the solidus and with rising temperature the vesicles contain fewer crystals (Fig. 4a).

In all of the experiments the amount of glass increases with rising temperature and pressure, to a maximum of 36 wt % at 1·5 GPa and 900°C (Fig. 3). The plagioclase content decreases with rising temperature and pressure, and plagioclase is not observed in the experiments at 1·5 GPa. The modal abundance of mafic silicates remains more or less constant at ~60 wt %. At 1·25 GPa and

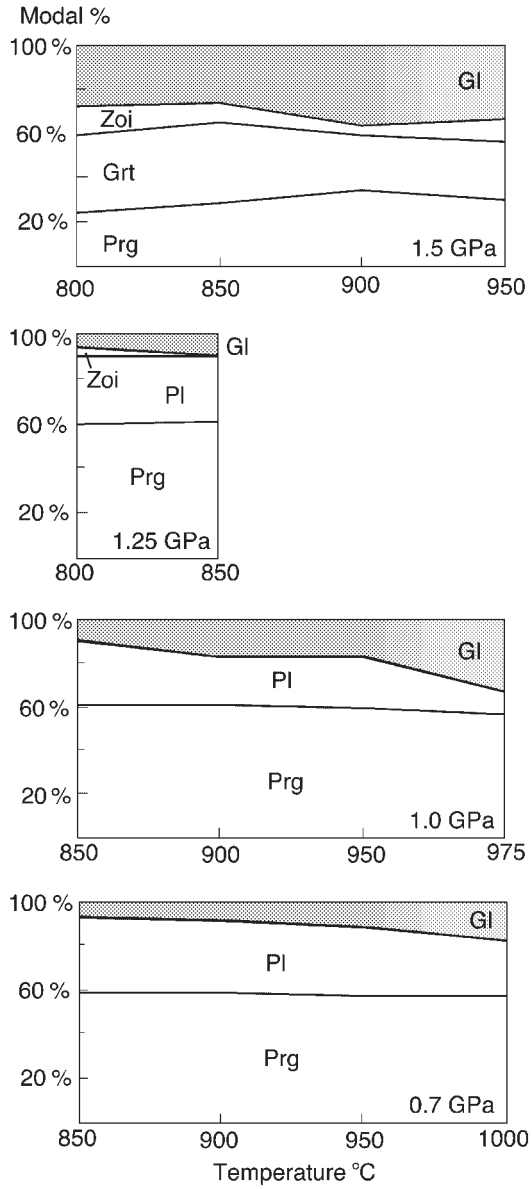

Fig. 3. Calculated modes in wt % vs temperature at 0·7, 1·0 and 1·5 GPa for the H_2O-saturated experiments. The modal compositions of the 1·25 GPa experiments were obtained from back-scattered electron images.

900°C and at higher *P–T*, amphibole decreases in amount whereas garnet appears and becomes more abundant with increasing pressure to a maximum of 36 wt % at 1·5 GPa and 900°C. The maximum content of zoisite in the experiments is 12 wt %.

PHASE COMPOSITIONS

Experimental glass composition

Glass compositions from all the H_2O-saturated experiments are presented in Table 5. Analyses are normalized to 100 wt %, but the original analytical totals are also given. The glasses in all the experiments contain numerous bubbles confirming H_2O saturation (Fig. 4c, f and h). Chemical analyses show that the glasses are homogeneous, and the SiO_2 content varies from 54·7 to 69·8 wt % (tonalitic to anorthositic) on an H_2O-free basis (Fig. 5). With rising temperature the abundances of SiO_2 and Na_2O decrease and CaO, FeO^t and MgO increase. Al_2O_3 shows a relatively flat but variable pattern (Fig. 5). The abundances of CaO and Al_2O_3 generally increase with increasing pressure from 0·5 to 1·25 GPa, but then decrease from 1·25 to 1·5 GPa. This reflects destabilization of the anorthite component with increasing pressure until zoisite precipitates at 1·5 GPa. The experiments at 1·25 GPa and 900 and 950°C are maximally enriched in the anorthite component (Fig. 5). This is also reflected in low Na_2O and SiO_2 abundances in these glasses. With increasing pressure to 1·5 GPa, the melts saturate in zoisite, which is reflected in a dramatic decrease in CaO and increase in Na_2O and SiO_2 (Fig. 5). Generally the near-solidus glass compositions at all pressures are similar, but then diverge at rising temperature. This reflects the different residual phases formed at the various pressures (Fig. 6).

The CIPW (wt %) normative feldspar composition of the experimentally produced glasses (Table 5) is plotted in the ternary system An–Ab–Or (Fig. 7). The glass compositions generally change from Ab rich to more An rich with rising temperature. The Or component is relatively constant, whereas total normalized plagioclase content in the glasses varies from 59 to 92%, showing that some of the glasses are anorthositic ($\geq$90 wt %) in composition (Table 5). All glasses are quartz normative, except in the three experiments with added Na(OH). The content of normative quartz in the glasses decreases with rising temperature.

The melts segregated and accumulated in the upper part of the capsules in the experiments at 1·0 GPa in the temperature range 900–975°C, 1·25 GPa at 900–950°C and 1·5 GPa at 950°C (Fig. 4c and h). This shows that the melts in these experiments had low viscosities and were highly mobile. This is consistent with the melt-drainage features in the SMC.

Amphibole

Amphibole is present in all the experiments either as euhedral prismatic crystals or as new mantles grown on relict amphibole grains (Fig. 4a, c and d). Average amphibole compositions are listed in Table 6 and these are pargasites following the nomenclature of Leake *et al.* (1997). The experimentally produced amphiboles

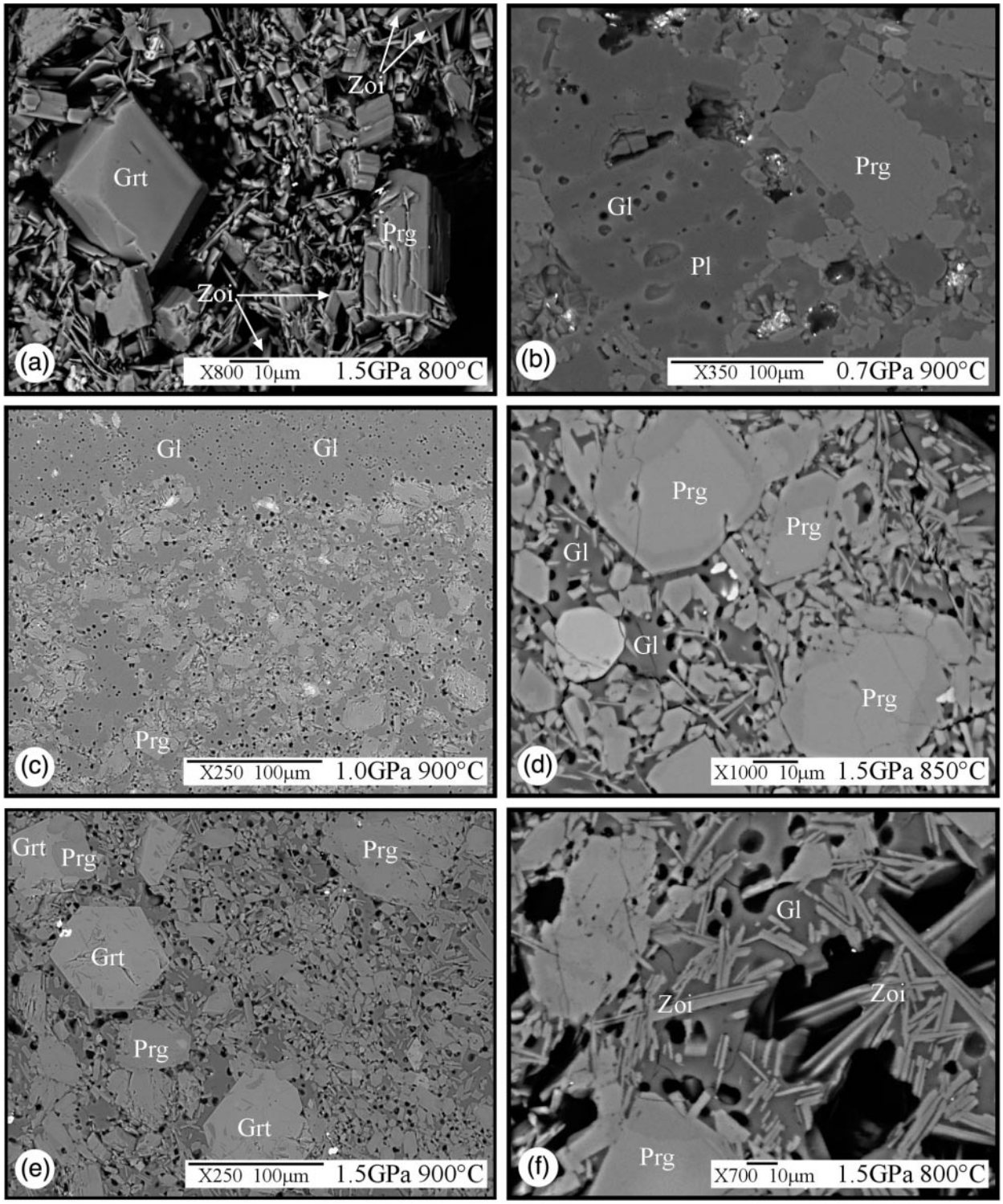

Fig. 4.

are similar in composition to amphiboles in the starting material at 0·5 and 0·7 GPa and close to the solidus in experiments at increasing pressures. At 1·25 and 1·5 GPa, Al increases and Fe decreases with rising temperature. There is also a weak decrease in Si with rising temperature at 1·0, 1·25 and 1·5 GPa.

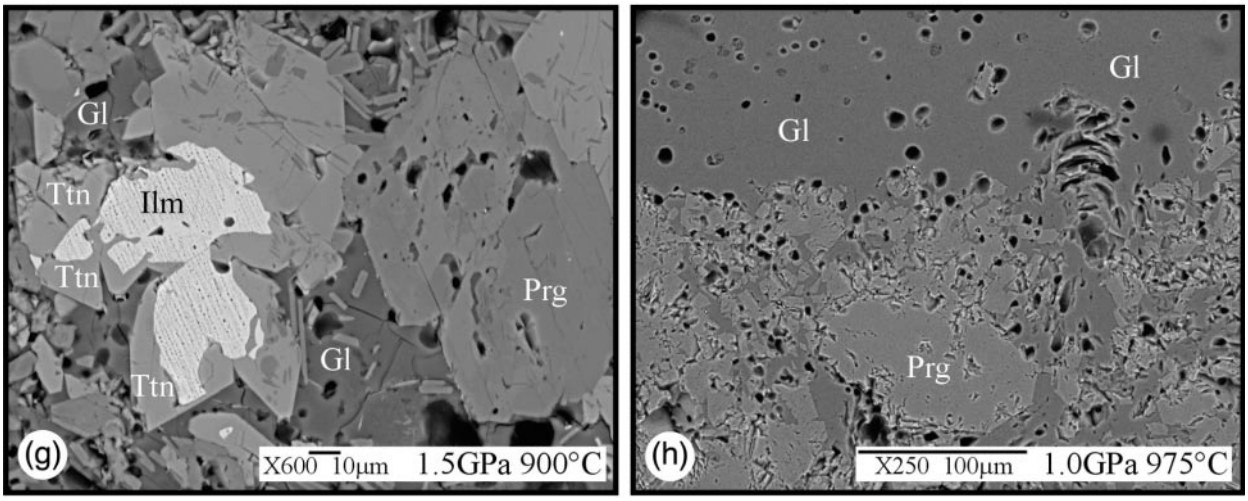

Fig. 4. Selected back-scattered electron photographs of selected experiments. (a) Vesicle filled with garnet (Grt), pargasite (Prg) and needles of zoisite (Zoi) at 1·5 GPa and 800°C. (b) Partly corroded plagioclase (Pl) with small amounts of glass (Gl) at 0·7 GPa and 900°C. (c) Experimentally produced glass and pargasite restite in the experiments at 1·0 GPa and 900°C. The layer of glass in the upper part of the capsule should be noted. (d) Amphibole is present in all experiments, and it occurs either as prismatic euhedral crystals or as mantles grown on relict amphibole grains. (e) Garnet crystals with inclusions of amphibole, indicating rapid growth of garnet. (f) Long prismatic needles of zoisite in the glass at 1·5 GPa and 800°C. (g) Titanite (Ttn) occurs as euhedral crystals along the margins of ilmenite (Ilm), and represents a reaction between the melt and the ilmenite. (h) Glass that has segregated and accumulated in the upper part of the capsule in the charges run at 1·0 GPa and 975°C. This indicates that the melts were highly mobile.

Garnet

Garnet is present as large euhedral crystals in all experiments at 1·5 GPa, and at 900 and 950°C at 1·25 GPa. The garnet crystals generally have inclusions of amphibole (Fig. 4e). The composition of the garnets is in the range $Grs_{46–48}$ $Alm_{33–35}$ $Prp_{16–17}$ for the experiment at 1·5 GPa and $Grs_{57–59}$ $Alm_{14–16}$ Prp_{26} at 1·25 GPa. This shows that the garnets at lower pressure and temperature are richer in the grossular component, but richer in almandine at higher pressure as a result of breakdown of amphibole and formation of abundant zoisite.

Zoisite

Zoisite occurs as euhedral prismatic needles in all the experiments at 1·5 GPa and at 800°C at 1·25 GPa (Fig. 4f). The average chemistry of the zoisite is (wt %) 39·4 SiO_2, 0·4 TiO_2, 31·2 Al_2O_3, 2·0 FeO^t, 0·3 MgO, 23·4 CaO, and zoisite shows very little chemical variation in the different experiments.

In one experiment (not listed) at 1·5 GPa and 950°C, which was H_2O rich but not H_2O saturated (5% H_2O added), zoisite was not observed. This shows that magmatic zoisite forms in melts with a high H_2O content in this system.

Ilmenite–titanite

Ilmenite is present in all the experiments as a relict phase. Titanite occurs usually as euhedral mantles on partly resorbed ilmenite grains (Fig. 4g). Formation of titanite is in accordance with the presence of titanite in the leucosomes and dykes in the SMC.

Plagioclase

Average plagioclase compositions in the residues vary from An_{70} to An_{84}. The plagioclase is always corroded because of melting (Fig. 4b), and the highest An contents are recorded in the experiments at the highest temperatures. In general, the plagioclase content decreases with rising temperature and pressure.

Clinopyroxene

Clinopyroxene (Cpx) has been observed as neoformed prismatic euhedral crystals in two experiments (1·0 GPa at 950 and 975°C). Beard & Lofgren (1991) observed Cpx in their water-saturated experiments of quartz-bearing amphibolites, but in much larger amounts.

INTERPRETATION OF EXPERIMENTAL RESULTS AND APPLICATION TO THE SMC

All the glasses in the experiments are rich in plagioclase components, which can be directly related to the preferential destabilization of plagioclase and stabilization of

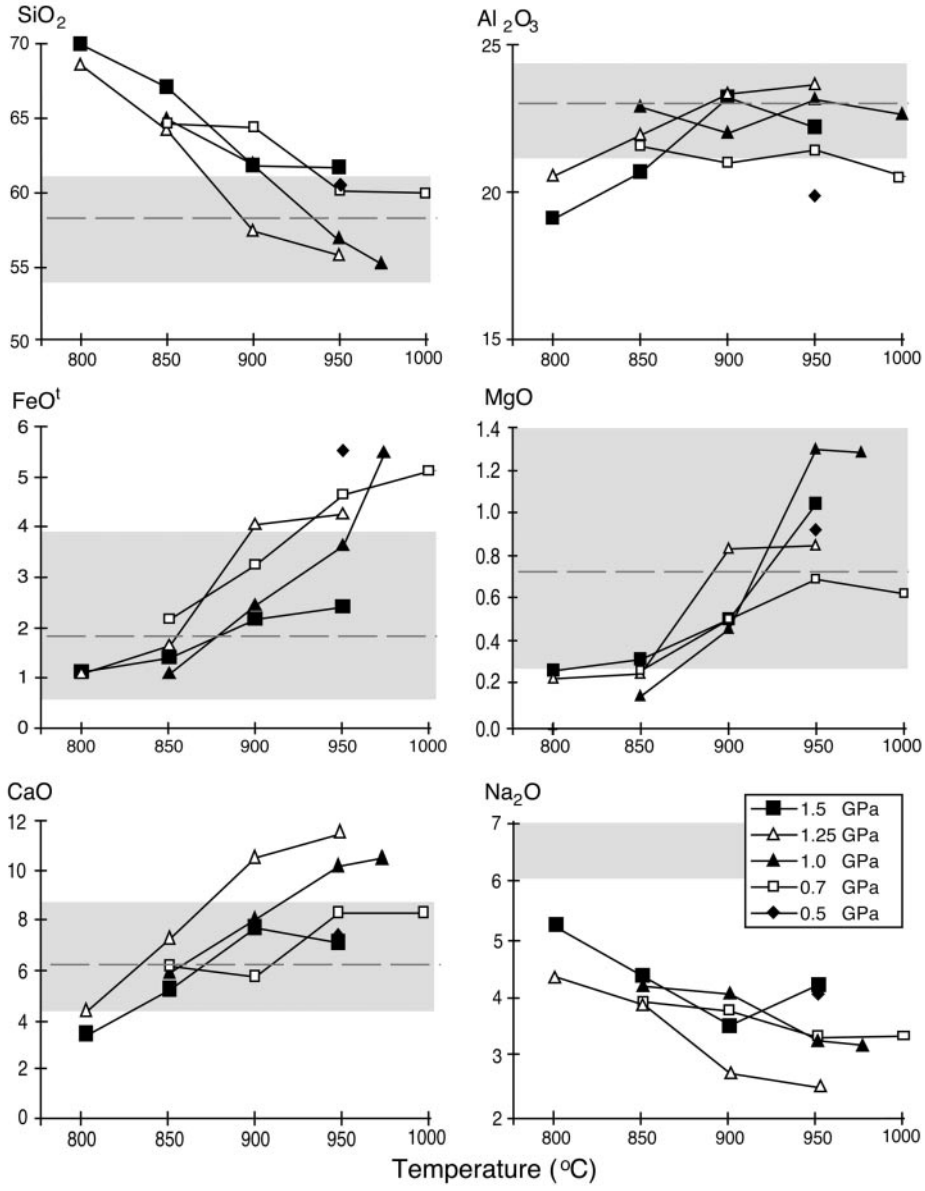

Fig. 5. Temperature–oxide wt % diagrams for experimental glasses with added H_2O. The grey fields cover the composition of the anorthosite dykes in the SMC. The dashed grey lines are average values for the dykes.

amphibole. This forms glasses that are rich in Al_2O_3 and CaO, and low in FeO^t, MgO and TiO_2. However, the residual phase assemblage varies with rising pressure and temperature, and this reflects the composition of the glasses.

On the basis of field relations and geochemistry the main melting reaction that probably occurred in the SMC is

$$\text{plagioclase} + H_2O = \text{melt} \qquad (1)$$

and this is supported by the experiments presented here.

The crystallization of zoisite with increasing pressure is important, as it limits the CaO content in the glass (Fig. 5). The formation of zoisite in the experiments at 1·25 GPa and 800°C and higher P–T is related to the breakdown of residual plagioclase under hydrous conditions:

$$4CaAl_2Si_2O_8 + H_2O = 2Ca_2Al_3Si_3O_{12}(OH) + Al_2O_3 + 2SiO_2$$

$$4 \text{ anorthite} + H_2O = 2 \text{ zoisite} + \text{melt} \qquad (2)$$

Table 5: Composition of experimentally produced glasses

P (GPa):	0·5	0·7	0·7	0·7	0·7	1·0	1·0	1·0	1·0	1·25	1·25	1·25	1·25	1·5	1·5	1·5	1·5
T (°C):	950	850	900	950	1000	850	900	950	975	800	850	900	950	800	850	900	950
SiO_2	60·55	64·71	64·55	60·20	60·40	64·73	61·76	56·71	54·65	68·39	63·98	57·31	55·60	69·78	66·92	61·63	61·52
TiO_2	0·54	0·60	—	0·28	0·27	—	0·06	0·60	0·74	—	—	0·22	0·73	—	0·01	0·18	0·21
Al_2O_3	19·93	21·60	21·07	21·52	20·75	22·94	22·05	23·24	22·74	20·60	22·02	23·38	23·73	19·12	20·73	23·25	22·29
FeO^t	5·54	2·19	3·29	4·68	5·17	1·13	2·48	3·68	5·50	1·12	1·69	4·09	4·31	1·15	1·43	2·20	2·44
MnO	0·18	0·14	0·14	0·14	0·22	0·06	0·11	0·14	0·16	0·08	0·01	0·16	0·10	0·04	0·10	0·05	0·06
MgO	0·93	0·28	0·52	0·71	0·64	0·16	0·47	1·31	1·30	0·24	0·26	0·85	0·86	0·28	0·33	0·52	1·06
CaO	7·57	6·38	5·93	8·57	8·49	6·10	8·33	10·41	11·09	4·52	7·47	10·75	11·71	3·55	5·44	7·79	7·30
Na_2O	4·09	3·93	3·78	3·30	3·34	4·21	4·08	3·26	3·17	4·37	3·88	2·69	2·44	5·25	4·37	3·52	4·23
K_2O	0·67	0·78	0·73	0·63	0·74	0·68	0·65	0·66	0·65	0·69	0·62	0·55	0·52	0·83	0·67	0·69	0·89
Total	87·26	85·40	84·36	86·46	85·33	88·00	84·85	85·50	85·14	86·73	86·25	84·76	86·10	88·68	88·61	85·28	86·00
CIPW																	
Q	14·2	23·8	24·1	16·5	16·4	23·6	15·7	10·0	7·0	29·6	21·6	13·5	12·1	27·3	25·8	19·4	14·9
C		2·7	3·3			4·2				4·5	1·4			3·1	2·9	2·2	1·1
Or	4·0	4·6	4·3	3·7	4·4	4·0	3·9	3·9	3·8	4·1	3·7	3·2	3·1	4·9	4·0	4·1	5·3
Ab	34·6	33·3	32·0	27·9	28·2	35·6	34·5	27·6	26·9	36·9	32·9	22·8	20·7	44·4	37·0	29·8	35·8
An	34·0	31·7	29·4	42·1	39·5	30·3	40·0	46·8	45·9	22·4	37·1	50·1	52·3	17·6	27·0	39·6	36·2
Total Pl	68·6	65·0	61·4	70·0	67·7	65·9	74·5	74·4	72·8	59·3	70·0	72·9	73·0	62·0	64·0	69·4	72·0
Di	3·0			0·4	2·3		1·2	4·0	7·7			2·8	5·0				
Hy	7·7	2·9	6·0	7·7	7·4	2·0	4·0	5·5	5·9	2·3	3·0	6·2	4·5	2·3	2·9	4·1	5·7
Mt	1·0	0·4	0·6	0·8	0·9	0·2	0·4	0·6	1·0	0·2	0·3	0·7	0·7	0·2	0·3	0·4	0·4
Il	1·0	1·1	0·5	0·5	0·1	1·1	1·4		0·4	1·4		0·3	0·4				

Table 5: continued

	2% Na(OH)					10% AL-1			
P (GPa):	0·7	1·0	1·0	1·0	1·25	0·7	0·7	1·0	1·0
T (°C):	900	850	900	950	900	850	900	850	900
SiO_2	58·94	61·59	57·72	58·78	60·11	62·09	59·34	61·51	59·77
TiO_2	—	—	0·02	0·01	0·02	—	0·51	—	0·32
Al_2O_3	25·86	23·67	24·45	24·34	23·33	22·54	22·13	22·91	23·28
FeO^t	0·96	1·10	2·16	2·06	2·14	2·16	3·23	1·87	2·97
MnO	0·04	0·08	0·01	0·08	0·09	0·05	0·17	0·10	0·09
MgO	0·08	0·15	0·32	0·32	0·31	0·35	1·08	0·32	0·84
CaO	3·14	3·78	6·35	7·45	6·26	7·16	8·39	7·89	9·35
Na_2O	10·38	9·11	8·25	6·27	7·15	5·28	4·67	5·03	2·90
K_2O	0·60	0·52	0·68	0·68	0·59	0·38	0·49	0·37	0·48
Total	89·80	87·32	88·27	87·76	89·11	87·45	85·97	88·05	84·48
CIPW									
Q	1·3			2·1		12·3	18·1	12·7	9·8
C		1·3			2·4		1·0	0·4	
Or	3·5	3·1	4·4	4·0	3·6	2·2	2·8	2·3	2·9
Ab	60·5	72·7	54·6	53·1	64·2	42·6	24·5	44·7	39·5
An	29·9	18·8	27·7	36·3	15·6	38·9	46·4	35·5	38·0
Total Pl	90·4	91·5	82·3	89·4	79·8	81·5	70·9	80·2	77·5
Ne		2·4	8·3		12·8				
Di	1·1		3·3	0·6		0·2			3·0
Hy	3·3			3·4		3·4	5·8	3·9	5·0
Ol		1·5	1·5		1·2				
Mt	0·4	0·2	0·4	0·4	0·2	0·3	0·5	0·4	0·6
Ilm							0·6		1·0

Reported analyses are average of 5–10 analyses of different glass pools. Q–C–Or–Ab–An–Di–Hy–Mt–Il, normative amounts of quartz–corundum–orthoclase–albite–anorthite–diopside–hypersthene–magnetite–ilmenite. FeO^t, total iron as FeO. Na(OH), experiments with 2 wt % Na(OH) added to the starting material; AL-1, experiments with 10 wt % albite standard AL-1 added to the starting material.

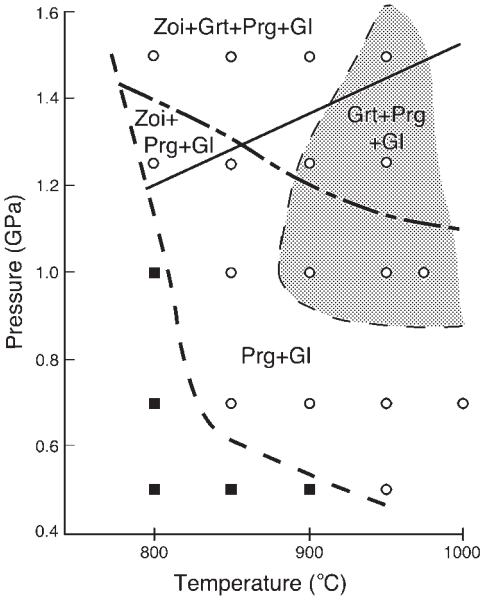

Fig. 6. Pressure–temperature diagram showing the experimental results from the sample 109SD. Open symbols represent experiments with glass present; filled symbols represent experiments with no detectable glass. The grey field covers those experiments that show melt segregation to the top of the capsule. Prg, pargasite; Grt, garnet; Zoi, zoisite; Gl, glass (Kretz, 1983). Ilmenite and plagioclase are relict phases and are not included in the phase diagram.

which will enrich the melt in SiO_2 (Fig. 5). However, zoisite also crystallizes directly from the H_2O-saturated melt, which will deplete the melt in Al_2O_3 and increase the melt SiO_2 content (Fig. 5). The occurrence of garnet is related to the breakdown of amphibole and the anorthite component of plagioclase with increasing pressure.

The experiments at 1·25 GPa and 1·5 GPa have residues that are incompatible with the field relationships in the SMC. No garnet or zoisite occurs in the amphibolitic restites, migmatites or the dykes. This suggests that the anorthosites in the SMC formed at a pressure lower than 1·25 GPa. The glasses at 0·7 GPa are too high in SiO_2 and FeO^t and too low in Al_2O_3 and Na_2O compared with the anorthositic dykes. The glass composition from the run at 900°C and 1 GPa most closely resembles the average anorthositic dyke composition in the SMC, but is too low in Na_2O and too high in SiO_2 (Tables 1 and 5, Fig. 5).

The sodium problem

The glasses in the water-saturated experiments contain less Na_2O than in the anorthositic dykes. This could possibly result either from (1) formation of the SMC by anatexis of a starting material that was richer in sodium than 109SD or (2) anatexis in the presence of a fluid phase that contained dissolved sodium. To test these alternatives we performed experiments with added albite and Na(OH).

Experiments with 10% added albite standard AL-1 did not produce nepheline-normative glasses, but glasses

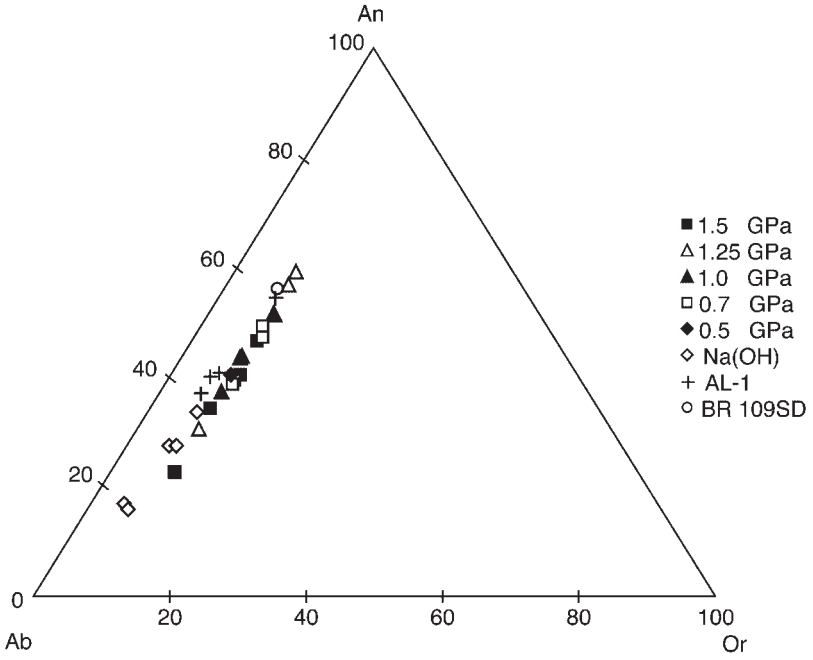

Fig. 7. An–Ab–Or plot based on the CIPW norms of all the experimentally produced glasses (Table 5). The glasses generally have higher An/Ab with increasing degree of melting.

Table 6: Representative composition of amphiboles (wt %)

P (GPa):	0·5	0·7	0·7	0·7	0·7	1·0	1·0	1·0	1·0	1·25	1·25	1·25	1·25	1·5	1·5	1·5	1·5	1·5
T (°C):	950	850	900	950	1000	850	900	950	975	800	850	900	950	800	850	900	950	950
SiO_2	40·47	41·11	41·45	42·08	40·85	40·94	39·68	38·43	39·12	40·76	40·87	37·60	37·95	41·37	41·40	40·10	39·06	
TiO_2	2·38	2·27	2·26	1·85	2·96	2·03	2·00	2·31	2·48	1·99	2·02	2·25	2·53	2·19	1·72	2·12	1·81	
Al_2O_3	12·95	13·16	13·24	12·93	13·96	13·78	15·45	15·11	15·52	13·35	14·22	18·54	18·22	13·39	15·16	15·85	18·80	
FeO†	14·80	15·77	15·65	14·88	12·96	15·47	14·56	14·36	14·28	15·34	15·19	12·91	13·39	15·29	13·87	14·51	12·32	
MnO	0·23	0·22	0·27	0·24	0·26	0·22	0·25	0·18	0·21	0·22	0·20	0·17	0·18	0·23	0·24	0·25	0·14	
MgO	9·90	9·56	9·85	10·29	10·69	9·31	9·33	10·26	9·66	9·68	9·59	9·49	9·55	9·82	9·67	9·33	10·01	
CaO	11·64	11·90	11·90	11·90	12·36	11·75	12·01	12·64	12·38	11·89	11·61	12·96	12·64	11·79	11·78	11·55	12·28	
Na_2O	2·35	2·38	2·42	2·35	2·55	2·45	2·63	2·79	2·48	2·30	2·43	2·73	2·67	2·39	2·63	2·83	2·98	
K_2O	0·85	0·91	0·89	0·94	0·59	0·82	0·65	0·46	0·68	1·01	0·90	0·51	0·55	0·91	0·71	0·63	0·46	
Total	95·60	97·13	97·93	97·46	97·18	96·77	96·55	96·54	96·81	96·54	97·03	97·16	97·67	97·37	97·17	97·15	97·86	

Table 6: continued

	Na(OH)					AL-1			
P (GPa):	0·7	1·0	1·0	1·0	1·25	0·7	0·7	1·0	1·0
T (°C):	900	850	900	950	900	850	900	850	900
SiO_2	41·17	41·04	41·32	40·63	40·88	39·72	39·88	41·50	39·73
TiO_2	1·89	1·93	2·15	2·01	2·02	2·63	2·08	2·16	2·22
Al_2O_3	12·99	13·73	13·46	15·36	13·65	12·99	14·50	11·95	14·59
FeO^t	15·21	15·23	15·23	15·01	15·70	15·42	13·68	15·55	14·59
MnO	0·27	0·34	0·27	0·16	0·25	0·41	0·24	0·12	0·19
MgO	9·96	9·35	9·68	9·50	9·70	9·01	9·28	9·63	9·95
CaO	11·51	11·68	11·67	12·00	11·82	11·34	11·51	11·37	12·01
Na_2O	2·33	2·59	2·73	2·71	2·49	2·28	2·53	2·25	2·48
K_2O	0·96	0·91	0·90	0·78	0·95	0·93	0·89	0·89	0·80
Total	96·29	97·41	97·41	98·16	97·46	94·73	94·56	95·42	96·56

Reported analyses are average of 7–10 analyses of different amphiboles. Na(OH), experiments with 2 wt % Na(OH) added to the starting material; AL-1, experiments with 10 wt % albite standard AL-1 added to the starting material.

slightly less quartz normative than the experiments with no added albite (Table 5). The sodium contents in the glasses were generally higher than in the experiments without added albite, but not as rich in Na as the dykes in the SMC. This indicates that the Na-rich nature of the dykes may result from the presence of a fluid with dissolved Na.

To study the effect on the glass composition by melting in the presence of a saline fluid, experiments were performed with 2% added Na(OH). Na_2O and CaO contents can also be affected by the composition of the fluid present. In the presence of a highly saline fluid phase (40–50 wt % $NaCl_{eq}$) most of the sodium in the fluid would enter the melt. If the host rock contains a minimum of 2–5% fluid when anatexis occurred, the glass will be enriched by 1–2 wt % Na_2O compared with a pure H_2O fluid. If the fluid had a lower salinity then more fluid is needed to produce the same enrichment of sodium in the glass. Fluid inclusions in plagioclase crystals from the anorthositic dykes contain three phases (liquid, solid and vapour). The solid phase is transparent, colourless and isotropic and is thus probably halite (NaCl). This indicates that the fluid causing the anatexis had a medium to high salinity. Fluid inclusions with salinities less than 30–35 wt % $NaCl_{eq}$ rarely nucleate halite crystals (Bodnar & Vityk, 1994).

The glasses produced in the water-saturated experiments with 2 wt % added Na(OH) are richer in plagioclase components and more enriched in Ab than glasses in the other experiments (Table 5). The glass produced at 1·0 GPa and 900°C has a major element composition that is indistinguishable from the dykes in the SMC (Tables 1 and 5). This experiment also exhibits an amphibole-rich and plagioclase-poor restite that is similar to that observed in the SMC. The glass in this experiment is also nepheline normative in contrast to most of the other experiments, suggesting that the rock may have been enriched in Na by a moderate- to high-salinity fluid during the anatexis.

In some of our experiments we added 10 wt % H_2O and 2 wt % Na(OH). This can be recalculated to a fluid with a salinity of 17 wt % [calculated as $Na(OH)_{eq}$] or 23 wt % (calculated as $NaCl_{eq}$). Medium- to high-salinity fluids are well known from subduction-zone environments and during exhumation and uplift during decompression (e.g. Scambelluri *et al.*, 1997; Markl & Bucher, 1998; Markl *et al.*, 1998; Scambelluri & Philippot, 2001; Selbekk *et al.*, 2002).

Melt segregation

Some of the experiments show that hydrous anorthositic melts can segregate after only 3 days, suggesting low melt viscosity and significant density contrast between the melt and the restite. High density contrast is demonstrated by the fact that oligoclase has a density of 2·66 g/cm^3 and pargasite a density of 3·2 g/cm^3 (Nickel & Nichols, 1991). An H_2O-saturated melt of oligoclase composition will have a lower density. The melt migration in the capsules must be related to the low viscosity of the melt and to the density contrast between the melt and the restite, as the pressure on the sample during the experiments is purely hydrostatic. It has also been suggested that the melt migration in the SMC is related to compaction based on the structural geology of the area (Skjerlie & Selbekk, 2000). The lowest P–T conditions where we observed melt migration in the capsule are at the same P–T as we suggest that the anorthositic melts formed, i.e. 1·0 GPa and 900°C (Figa 4f and 6). This may explain the high amount of dykes in the SMC, and the very effective melt drainage in the migmatites.

TECTONOMAGMATIC MODEL

The tectonic setting during the formation of the SMC is at present unknown. The host rock to the SMC was probably a layered mafic igneous complex of unknown age. The association of alkaline gabbroic rocks with surrounding quartzo-feldspathic metasedimentary rocks may, however, suggest a continental rift setting (e.g. Wilson, 1989).

The age of the anorthositic dykes and the leucosomes in the SMC falls between two periods when island arcs and marginal basins formed along the Iapetus margin at 500–469 Ma and 445–435 Ma (e.g. Pedersen *et al.*, 1988, 1991). According to current models, ophiolites related to the 500–469 Ma event (Group I) were obducted onto the continental margin before the 445–435 Ma event (Pedersen *et al.*, 1988, 1991). The age of the SMC fits with the suggested time of emplacement (450–460 Ma) of island-arc complexes onto the Laurentian margin related to westward subduction (Pedersen *et al.*, 1988). After or during obduction of the Group I ophiolites, the continental margin was thickened and eclogites formed in the Tromsdalstind sequence.

The SMC formed during a period of uplift, retrogression and hydrous partial melting of the eclogites and related rocks in the Tromsdalstind sequence. This is demonstrated by the 458 Ma date on a pegmatite related to partial melting of the eclogites in the Tromsdalstind sequence during exhumation of this complex (K. P. Skjerlie, personal communication, 2001). The SMC is cross-cut by anorthosite dykes of the same composition as the leucosome, suggesting increasing melting depth with time. During uplift progressively deeper-seated rocks will melt as they rise and cross the solidus (Fig. 8). Thus, rocks will melt, cool, and then be intruded by melts formed below. We speculate that this scenario may be

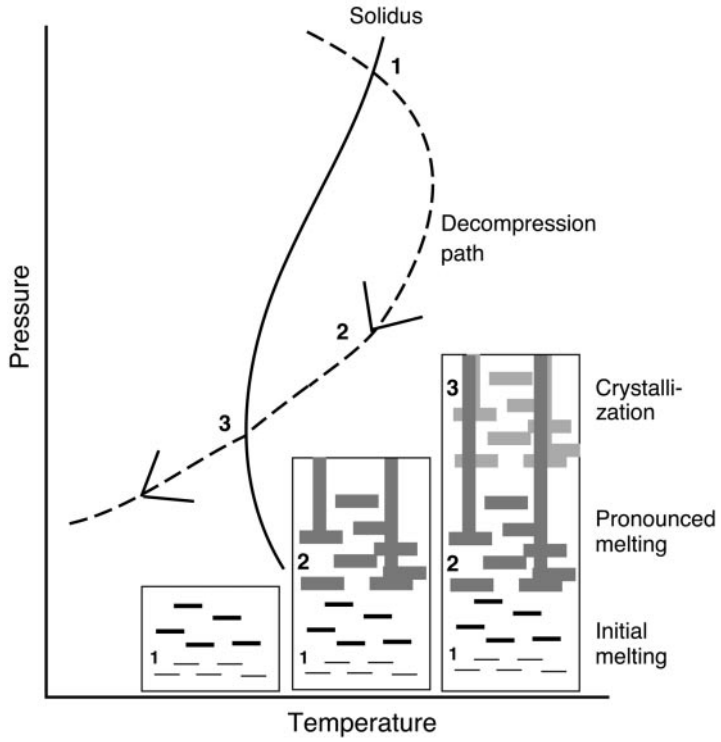

Fig. 8. *P–T* diagram showing how moderate-rate decompression may cause progressively deeper-seated rocks to melt. The SMC is cross-cut by anorthosite dykes of the same composition as the leucosome, suggesting increasing melting depth with time. During uplift progressively deeper-seated rocks will melt as they rise and cross the solidus (1). Thus, rocks will melt (1 and 2), cool, and then be intruded by melts formed below (3). We speculate that this scenario may be responsible for the formation of the SMC.

responsible for the formation of the SMC. If this model is correct, the highly saline fluids could have originated from the dehydration of the deeper-seated eclogites and related rocks of the Tromsdalstind sequence.

CONCLUSIONS

Field evidence, geochemistry and the melting experiments reported here suggest that anorthositic liquids can form in nature by anatexis of nepheline-normative mafic rocks in the presence of an H_2O-bearing fluid phase. The experiments show that a variety of melt compositions from tonalite to anorthosite can be produced at different conditions. An important result of these experiments is that the glasses have a very high proportion of plagioclase components (up to 92 wt %).

The experiments suggest that the anorthositic dykes in the SMC probably formed by anatexis of alkaline gabbro in the presence of an H_2O-bearing fluid phase at about 1·0 GPa and 900–950°C. To explain the sodic and nepheline-normative rocks of the SMC, excess sodium is probably needed. It is suggested that the H_2O-bearing fluid causing the anatexis was moderately to highly saline, and our experimentally produced glasses with 2% Na(OH) added at 1·0 GPa and 900°C are indistinguishable from the anorthosites in the SMC. The limited *P–T* area where anorthositic melts are produced indicates that hydrous anatectic anorthosites probably are rare in nature. Our experiments indicate that hydrous anorthositic melts are highly mobile. This can explain the high abundance of dykes in the SMC.

ACKNOWLEDGEMENTS

This work was supported by funding from the University of Tromsø and the Norwegian Research Council (project code 128158/410). We wish to thank Professor Brian Robins for providing the sample for the experimental work and for reading through an early version of the manuscript. Dr Muriel Erambert and Professor Håkon Austrheim are thanked for help with the microprobe analyses. The journal reviewers Professor Ronald Frost, Professor Gregor Markl and a anonymous reviewer provided constructive criticism, which improved the paper substantially.

REFERENCES

Andresen, A., Fareth, E., Bergh, S., Kristensen, S. E. & Krogh, E. J. (1985). Review of Caledonian lithotectonic units in Troms, North Norway. In: Gee, D. G. & Sturt, B. A. (eds) *The Caledonian Orogeny—Scandinavia and Related Areas*. Chichester: John Wiley, pp. 569–578.

Ashwal, L. D. (1993). Anorthosites. In: *Minerals and Rocks*, *21*. Berlin: Springer, 422 pp.

Ashworth, J. R. (1985). Introduction. In: Ashworth, J. R. (ed.) *Migmatites*. Glasgow: Blackie, 302 pp.

Beard, J. S. & Lofgren, G. E. (1989). Effect of water on the composition of melts of greenstone and amphibolites. *Science* **244**, 195–197.

Beard, J. S. & Lofgren, G. E. (1991). Dehydration melting and water-saturated melting of basaltic and andesitic greenstone and amphibolites at 1, 3, and 6·9 kb. *Journal of Petrology* **32**, 365–401.

Binns, R. E. (1978). Caledonian nappe correlation and orogenic history in Scandinavia north of lat 67°N. *Geological Society of America Bulletin* **89**, 1475–1490.

Bjørlykke, A. & Olaussen, S. (1981). Silurian sediments, volcanics and mineral deposits in the Sagelvvatn area, Troms, Northern Norway. *Norges Geologiske Undersøkelse* **365**, 39–54.

Bodnar, R. J. & Vityk, M. O. (1994). Intepretation of microthermometric data for H_2O–NaCl fluid inclusions. In: De Vivo, B. & Frezzotti, M. L. (eds) *Fluid Inclusions in Minerals: Methods and Applications*. Blacksburg, VA, USA: Virginia Polytechnic Institute and State University, pp. 117–130.

Conrad, W. K., Nicholls, I. A. & Wall, V. J. (1988). Water-saturated and undersaturated melting of metaluminous and peraluminous crustal compositions at 10 kb: evidence for the origin of silicic magmas in the Taupo volcanic zone, New Zealand, and other occurrences. *Journal of Petrology* **29**, 765–803.

De Waard, D. (1969). The anorthosite problem: the problem of the anorthosite–charnockite suite of rocks. *New York State Museum Science Service Memoirs* **18**, 71–90.

Duchesne, J. C., Liègeois, J. P., Vander Auwera, J. & Longhi, J. (1999). The crustal tongue melting model and the origin of massive anorthosites. *Terra Nova* **11**, 100–105.

Emslie, R. F. (1985). Proterozoic anorthosite massifs. In: Tobin, A. C. & Touret, J. L. R. (eds) *The Deep Proterozoic Crust in the North Atlantic Provinces*. Dordrecht: D. Reidel, pp. 39–60.

Fershater, G. B., Bea, F., Borodina, N. S. & Montero, M. P. (1998). Anatexis of basites in a paleosubduction zone and the origin of anorthosite–plagiogranite series of the Ural platinum-bearing belt. *Geochemistry International* **36**, 684–697.

Fram, M. S. & Longhi, J. (1992). Phase equilibria of dikes associated with Proterozoic anorthosite complexes. *American Mineralogist* **77**, 605–616.

Furnes, H. & Pedersen, R. B. (1995). The Lyngen Magmatic Complex: geology and geochemistry. *Geonytt* **22**, 30.

Govindaraju, K. (1984). Compilation of working values and sample description of 170 international reference samples of mainly silicate rocks and minerals. *Geostandards Newsletter* **8**, *Special July issue*, 1–91.

Govindaraju, K. (1989). Compilation of working values and sample description for 272 geostandards. *Geostandards Newsletter* **13**, *special issue*, 113 pp.

Hall, A. (1987). *Igneous Petrology*. Harlow, UK: Longman, 573 pp.

Housh, T. B. & Luhr, J. F. (1991). Plagioclase–melt equilibria in hydrous systems. *American Mineralogist* **76**, 477–492.

Jafri, S. H. & Saxena, R. (1981). Geochemistry of anorthositic dyke from Nuggihalli schist belt of Dharwar Craton, Karnataka, India. *Journal of the Geological Society of India* **22**, 85–91.

Johannes, W. (1978). Melting of plagioclase in the system Ab–An–H_2O and Qz–Ab–An–H_2O at P_{H_2O} = 5 kbars, an equilibrium problem. *Contributions to Mineralogy and Petrology* **66**, 295–303.

Johannes, W. & Holtz, F. (1996). Petrogenesis and experimental petrology of granitic rocks. In: *Minerals and Rocks*, *22*. Berlin: Springer, 335 pp.

Kolderup, C. F. (1933). The anorthosites of western Norway. *XVI International Geological Congress, Washington, DC* **1**, 289–294.

Kretz, R. (1983). Symbols for rock-forming minerals. *American Mineralogist* **68**, 277–279.

Krogh, E. J., Andresen, A., Bryhni, I., Broks, T. M. & Kristensen, S. E. (1990). Eclogites and polyphase *P–T* cycling in the Caledonian Uppermost Allochthon in Troms, northern Norway. *Journal of Metamorphic Geology* **8**, 289–309.

Landmark, K. (1951). Dykes of oligoclasite in amphibolite near Tromsø. *Acta Borealia* **1**, 3–23.

Landmark, K. (1973). Beskrivelse til de geologiske kart 'Tromsø' og 'Målselv'. II Kaledonske bergarter. *Tromsø Museums Skrifter* **15**, 1–263.

Leake, B. E., Woolley, A. R., Arps, C. E. S., Birch, W. D., Gilbert, M. C., Grice, J. D., Hawthorne, F. C., Kato, A., Kisch, H. J., Krivovichev, V. G., Linthout, K., Laird, J., Mandarino, J. A., Maresch, W. V., Nickel, E. H., Rock, N. M. S., Schumacher, J. C., Smith, D. C., Stephenson, N. C. N., Ungaretti, L., Whittaker, E. J. W. & Youzhi, G. (1997). Nomenclature of amphiboles: Report of the Subcommittee on Amphiboles of the International Mineralogical Association, Commission on New Minerals and Mineral Names. *American Mineralogist* **82**, 1019–1037.

Leelanandam, C. & Reddy, Y. J. (1990). Anorthosite dyke from the Pasupugallu gabbro pluton, Prakasam district, Andhra Pradesh, India. *Current Science* **59**, 105–107.

Longhi, J., Vander Auwera, J., Fram, M. S. & Duchesne, J. C. (1999). Some phase equilibrium constraints on the origin of Proterozoic (Massif) anorthosites and related rocks. *Journal of Petrology* **40**, 339–362.

Markl, G. & Bucher, K. (1998). Composition of fluids in the lower crust inferred from metamorphic salt in lower crustal rocks. *Nature* **391**, 781–783.

Markl, G., Ferry, J. & Bucher, K. (1998). Formation of saline brines and salt in the lower crust by hydration reactions in partially retrogressed granulites from the Lofoten Islands, Norway. *American Journal of Science* **298**, 705–757.

Mehnert, K. R. (1968). *Migmatites and the Origin of Granitic Rocks*. Amsterdam: Elsevier, 393 pp.

Nickel, E. H. & Nichols, M. C. (1991). *Mineral Reference Manual*. New York: Van Nostrand Reinhold, 250 pp.

Oliver, G. J. H. (1977). Feldspathic hornblende and garnet granulites and associated anorthosite pegmatites from Doubtful Sound, Fiordland, New Zealand. *Contributions to Mineralogy and Petrology* **65**, 111–121.

Oliver, G. J. H. & Krogh, T. (1995). U–Pb zircon age of 4690 ± 5 Ma for the Kjosen unit of the Lyngen magmatic complex, northern Norway. *Norges Geologiske Undersøkelses Bulletin* **428**, 27–33.

Patiño Douce, A. E. & Beard, J. S. (1995). Dehydration-melting of biotite gneiss and quartz amphibolite from 3 to 15 kbar. *Journal of Petrology* **36**, 707–738.

Patiño Douce, A. E. & Beard, J. S. (1996). Effects of *P*, f_{O_2} and Mg/Fe ratio on dehydration melting of model metagreywackes. *Journal of Petrology* **37**, 999–1024.

Patiño Douce, A. E. & Harris, N. (1998). Experimental constraints on Himalayan anatexis. *Journal of Petrology* **39**, 689–710.

Pedersen, R. B., Furnes, H. & Dunnings, G. R. (1988). Some Norwegian ophiolite complexes reconsidered. *Norges Geologiske Undersøkelses Special Publications* **3**, 80–85.

Pedersen, R. B., Furnes, H. & Dunnings, G. R. (1991). A U/Pb age for the Sulitjelma Gabbro, North Norway: further evidence for the development of a Caledonian marginal basin in Ashgill–Llandovery time. *Geological Magazine* **128**, 141–153.

Robins, B. (1982). The geology and petrology of the Rognsund Intrusion, West Finnmark, Northern Norway. *Norges Geologiske Undersøkelse* **371**, 1–55.

Scambelluri, M. & Philippot, P. (2001). Deep fluids in subduction zones. *Lithos* **55**, 213–227.

Scambelluri, M., Piccardo, G. B., Philippot, P., Robbiano, A. & Negretti, L. (1997). High salinity inclusions formed from recycled seawater in deeply subducted alpine serpentinite. *Earth and Planetary Science Letters* **148**, 485–499.

Selbekk, R. S., Furnes, H. Pedersen, R. B. & Skjerlie, K. P. (1998). Contrasting tonalite genesis in the Lyngen Magmatic Complex, north Norwegian Caledonides. *Lithos*, **42**, 243–268.

Selbekk, R. S., Skjerlie, K. P. & Pedersen, R. B. (2000). Generation of anorthositic magma by H_2O-fluxed anatexis of silica-undersaturated gabbro: an example from the north Norwegian Caledonides. *Geological Magazine* **137**, 609–621.

Selbekk, R. S., Bray, C. & Spooner, E. T. C. (2002). Formation of tonalite in island arcs by seawater-induced anatexis of mafic rocks; evidence from the Lyngen Magmatic Complex, North Norwegian Caledonides. *Chemical Geology* **182**, 69–84.

Simmons, E. C. & Hanson, G. N. (1978). Geochemistry and origin of massif-type anorthosites. *Contributions to Mineralogy and Petrology* **66**, 119–135.

Skjerlie, K. P. & Selbekk, R. S. (2000). Compaction-controlled migration of anatectic anorthositic melt in the Skattøra Migmatite Complex of North Norway. *EOS Transactions, American Geophysical Union* **81**, *Fall Meeting Supplement* V71A-13 (F1293).

Taylor, R. S., Campbell, I. H. McCulloch, M. T. & McLennan, S. M. (1984). A lower crustal origin for massif type anorthosites. *Nature* **311**, 372–374.

Wiebe, R. A. (1979). Anorthositic dykes in southern Nain Complex, Labrador. *American Journal of Science* **279**, 394–410.

Wilson, M. (1989). *Igneous Petrogenesis*. London: HarperCollins, 466 pp.

Yoder, H. S. & Tilley, C. E. (1962). Origin of basalt magmas; an experimental study of natural and synthetic rock systems. *Journal of Petrology* **3**, 342–532.

Zwaan, B. K., Fareth, E. & Grogan, P. W. (1998). Geologisk kart over Norge, Bergrunnskart Tromsø M 1:250 000. Norges Geologiske Undersøkelse, Trondheim.